

# Secreted Frizzled-Related Protein 3 Regulates Activity-Dependent Adult Hippocampal Neurogenesis

Mi-Hyeon Jang,<sup>1,2,5,8,\*</sup> Michael A. Bonaguidi,<sup>1,2,8</sup> Yasuji Kitabatake,<sup>1,2,6,8</sup> Jiaqi Sun,<sup>1,7,8</sup> Juan Song,<sup>1,2</sup> Eunchai Kang,<sup>1,2</sup> Heechul Jun,<sup>1,5</sup> Chun Zhong,<sup>1,2</sup> Yijing Su,<sup>1,2</sup> Junjie U. Guo,<sup>1,3</sup> Marie Xun Wang,<sup>1</sup> Kurt A. Sailor,<sup>1,3</sup> Ju-Young Kim,<sup>1,2</sup> Yuan Gao,<sup>1,4</sup> Kimberly M. Christian,<sup>1,2</sup> Guo-li Ming,<sup>1,2,3</sup> and Hongjun Song<sup>1,2,3,\*</sup>

<sup>1</sup>Institute for Cell Engineering

<sup>2</sup>Department of Neurology

<sup>3</sup>The Solomon H. Snyder Department of Neuroscience

<sup>4</sup>Lieber Institute for Brain Development

Johns Hopkins University School of Medicine, Baltimore, MD 21205, USA

<sup>5</sup>Department of Neurologic Surgery, Department of Biochemistry and Molecular Biology, Mayo College of Medicine, Rochester, MN 55905, USA

<sup>6</sup>Department of Pediatrics, Osaka University School of Medicine, 2-2 Yamadaoka, Suita, Osaka 565-0871, Japan

<sup>7</sup>School of Life Sciences, Tsinghua University, Beijing 100081, P.R. China

<sup>8</sup>These authors contributed equally to this work

\*Correspondence: [jang.mihyeon@mayo.edu](mailto:jang.mihyeon@mayo.edu) (M.-H.J.), [shongju1@jhmi.edu](mailto:shongju1@jhmi.edu) (H.S.)

<http://dx.doi.org/10.1016/j.stem.2012.11.021>

## SUMMARY

Adult neurogenesis, the process of generating mature neurons from adult neural stem cells, proceeds concurrently with ongoing neuronal circuit activity and is modulated by various physiological and pathological stimuli. The niche mechanism underlying the activity-dependent regulation of the sequential steps of adult neurogenesis remains largely unknown. Here, we report that neuronal activity decreases the expression of secreted frizzled-related protein 3 (sFRP3), a naturally secreted Wnt inhibitor highly expressed by adult dentate gyrus granule neurons. *Sfrp3* deletion activates quiescent radial neural stem cells and promotes newborn neuron maturation, dendritic growth, and dendritic spine formation in the adult mouse hippocampus. Furthermore, *sfrp3* reduction is essential for activity-induced adult neural progenitor proliferation and the acceleration of new neuron development. Our study identifies sFRP3 as an inhibitory niche factor from local mature dentate granule neurons that regulates multiple phases of adult hippocampal neurogenesis and suggests an interesting activity-dependent mechanism governing adult neurogenesis via the acute release of tonic inhibition.

## INTRODUCTION

In the adult mammalian brain, active neurogenesis arises from neural stem cells in the subgranular zone (SGZ) of the dentate gyrus (Ming and Song, 2011). Radial glia-like precursors (RGLs) within the SGZ serve as one type of quiescent neural stem cell

and continuously give rise to both dentate granule neurons and astrocytes in the adult mouse dentate gyrus (Bonaguidi et al., 2012). It is generally believed that the local neurogenic niche both houses neural stem cells and regulates their development. A number of niche components have been proposed, including blood vessels, astrocytes, ependymal cells, and mature neurons (Ming and Song, 2011). For example, hippocampal astrocytes have been shown to instruct the neuronal fate of cultured adult neural progenitors via Wnt signaling (Lie et al., 2005; Song et al., 2002). Lentivirus-mediated blockade of Wnt signaling reduces the number of immature new neurons in the adult dentate gyrus and impairs hippocampus-dependent spatial- and object-recognition memory (Jessberger et al., 2009). Dysfunctional Wnt signaling also has been implicated in the age-related decline of hippocampal neurogenesis (Miranda et al., 2012). The endogenous Wnt ligands and inhibitors that are responsible for niche regulation of adult neurogenesis remain unclear.

Different from other somatic stem cell compartments, adult hippocampal neurogenesis proceeds concurrently with the ongoing activity of existing neuronal circuits and is regulated by many physiological and pathological stimuli that affect neuronal activity, such as an enriched environment, physical exercise, specific learning tasks, and seizures (Ming and Song, 2011). For instance, seizures promote proliferation of adult dentate neural progenitors (Madsen et al., 2000; Parent et al., 1997) and accelerate the maturation and integration of newborn neurons (Overstreet-Wadiche et al., 2006). These studies suggest the presence of stimulators and/or inhibitors that balance the magnitude and rate of adult neurogenesis in response to changes in existing neuronal-circuit activity. The molecular identities of extrinsic factors, their niche sources, and the cellular targets that link circuit activity to adult neurogenesis are largely unknown.

Searching for activity-dependent extrinsic regulators of adult neurogenesis, we performed RNA-sequencing (RNA-seq) analysis of adult mouse dentate gyri with or without electroconvulsive

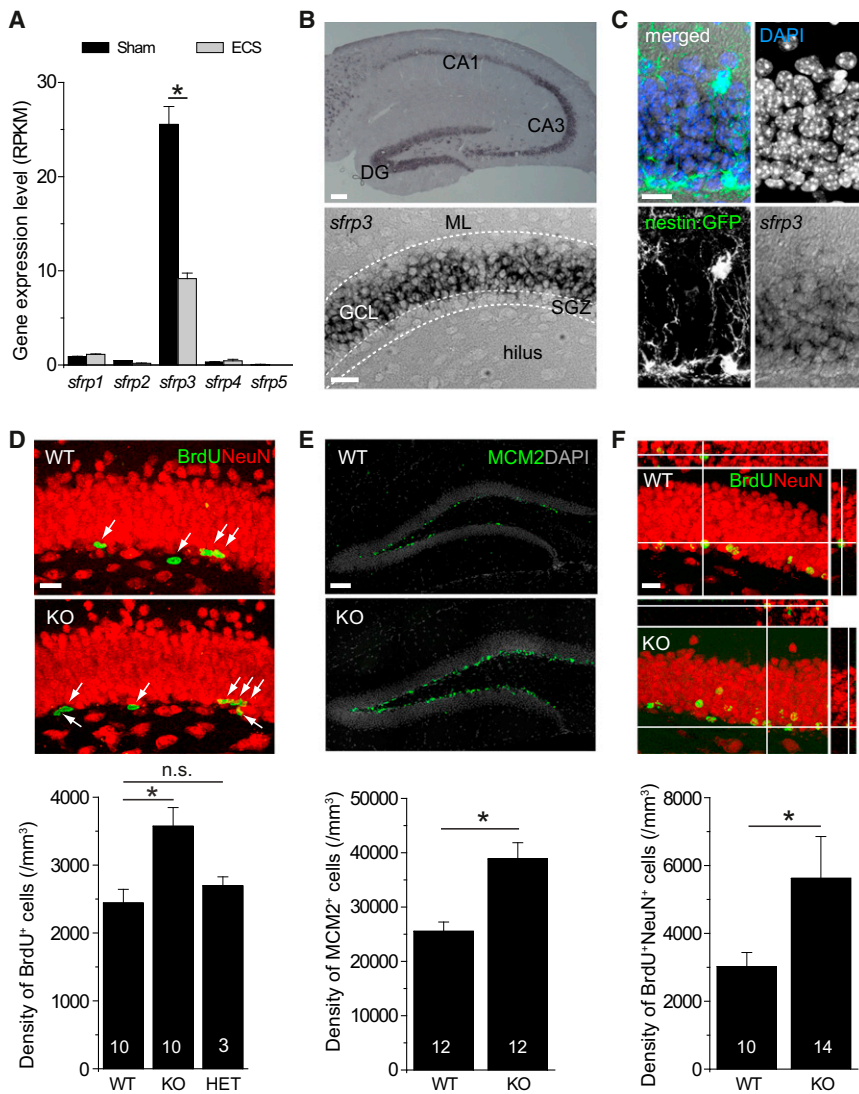


**Figure 1. *sfrp3* Expression and Regulation of Neurogenesis in the Adult Hippocampus**

(A) RNA-seq quantification of *sfrp1–sfrp5* expression in microdissected dentate gyri of adult wild-type (WT) mice 0 or 4 hr after a single ECS. Values represent mean  $\pm$  SEM (n = 3; \*, p < 0.01; one-way ANOVA). RPKM, reads per kilobase of exon per million fragments mapped.

(B and C) *sfrp3* expression in the adult mouse hippocampus. Shown in (B) are sample in situ images of *sfrp3* expression in the whole hippocampus (top; scale bar represents 100  $\mu$ m) and dentate gyrus (bottom; scale bar represents 20  $\mu$ m). Note *sfrp3* expression in the granule cell layer (GCL) but not in the SGZ (bottom). ML, molecular layer. Shown in (C) are sample dual *sfrp3* in situ and GFP immunostaining of the dentate gyrus of adult *nestin-GFP* mice. Scale bars represent 20  $\mu$ m.

(D–F) Increased progenitor proliferation and newborn neuron number in the dentate gyrus of adult *sfrp3* KO mice. In (D), animals were injected with BrdU and analyzed 2 hr later. Shown are sample projected confocal images of BrdU immunostaining (arrows) in the dentate gyrus of adult *sfrp3* KO and WT littermates (top; scale bar represents 50  $\mu$ m) and the stereological quantification of BrdU<sup>+</sup> cells in the SGZ of adult WT, HET, and KO littermates (bottom). The number associated with bar graphs indicates the number of animals examined. Values represent mean  $\pm$  SEM (\*, p < 0.01; n.s., p > 0.1; one-way ANOVA). Shown in (E) are sample projected confocal images of MCM2 immunostaining and DAPI staining in the dentate gyrus (top; scale bar represents 100  $\mu$ m) and stereological quantification of MCM2<sup>+</sup> cells. Values represent mean  $\pm$  SEM (\*, p < 0.05; Student's t test). In (F), adult mice were injected with BrdU once daily for 1 week and examined 4 weeks after the first BrdU injection. Shown are sample projected confocal images of BrdU and NeuN immunostaining (top). Orthogonal views are shown to confirm colocalization of BrdU and NeuN. Scale bar represents 50  $\mu$ m. Also shown is the stereological quantification of NeuN<sup>+</sup>BrdU<sup>+</sup> mature newborn neurons (bottom). Values represent mean  $\pm$  SEM (\*, p < 0.01; Student's t test). See also Figure S1 and Table S1.

stimulation (ECS), a paradigm that stimulates dentate circuits and promotes progenitor proliferation and new neuron development during adult hippocampal neurogenesis (Ma et al., 2009; Madsen et al., 2000; Zhao et al., 2012). We found that the level of secreted frizzled-related protein 3 (*sfrp3*), a gene highly expressed in the adult dentate gyrus, was significantly reduced by ECS (Figure 1A). Members of the sFRP family (sFRP1–sFRP5) can bind extracellular Wnt and thereby inhibit Wnt signaling (Jones and Jomary, 2002). Wnt signaling regulates diverse developmental processes in the embryonic brain and controls the proliferation and differentiation of progenitors in various adult tissues, including gut tissue, hair follicles, bone, blood, and nervous systems (Clevers and Nusse, 2012). Many Wnts retain their expression in the adult dentate gyrus (Shimogori et al., 2004). In this study, we identify sFRP3 as an important inhibitory niche factor arising from mature dentate granule neurons to regulate neural stem cell quiescence

and control the tempo of new neuron maturation in the adult hippocampus in an activity-dependent fashion.

## RESULTS

### sFRP3 Limits Dentate Neural Progenitor Proliferation and New Neuron Production

To identify activity-dependent extrinsic regulators of adult neurogenesis, we examined the expression profiles of all known Wnt inhibitors in microdissected adult dentate gyrus tissue, including the sFRP family (Figure 1A), Dickkopf family (*Dkk1–Dkk4*), Wnt inhibitor factor (*Wif1*), and Cerberus (*Cer1*; Figure S1A, available online). Notably, RNA-seq showed high levels of *sfrp3* and *Dkk3* expression, but only *sfrp3* expression was significantly altered by ECS. In situ analysis revealed specific and high levels of *sfrp3* expression in the dentate granule cell layer, but not the

SGZ, of adult mice (Figure 1B), whereas high levels of *Dkk3* expression were limited to nearby CA3 neurons (Thompson et al., 2008). In adult *nestin-GFP* transgenic mice, minimal *sfrp3* expression was detected in GFP<sup>+</sup> neural progenitors and their immature progeny in the adult dentate gyrus (Figure 1C), a result consistent with recent expression profiling of purified neural progenitors and immature neurons from adult mouse dentate gyri (Bracko et al., 2012).

To assess the potential role of sFRP3 in adult hippocampal neurogenesis, we obtained *sfrp3* knockout (KO) mice (Figure S1B). Adult *sfrp3* heterozygous (HET) and homozygous KO mice were grossly normal without any detectable developmental defects (data not shown). For the labeling of cells during the S phase of the cell cycle, adult mice were intraperitoneally (i.p.) injected once with BrdU (200 mg/kg body weight), and they were sacrificed 2 hr later. Stereological quantification showed a significant increase in the BrdU<sup>+</sup> cell density in the SGZ of adult *sfrp3* KO mice compared to wild-type (WT) or HET littermates (Figure 1D). Analysis with the endogenous cell proliferation marker MCM2 showed similar results (Figure 1E). To rule out potential developmental contributions from *sfrp3* germ-line deletion, we developed lentiviruses and adeno-associated viruses (AAVs) to acutely knock down endogenous sFRP3 expression in adult WT mice (Figure S1C). Fourteen days after stereotaxic injection of lentiviruses coexpressing small hairpin RNA (shRNA)-*sfrp3* and tdTomato fluorescent protein into the dentate gyrus, stereological quantification showed a significant increase of BrdU<sup>+</sup> cells in the SGZ compared to shRNA-control cells (Figure S1D). Consistent with the notion that sFRP3 inhibits Wnt signaling (Jones and Jomary, 2002), TOPGAL reporter mice, which express a LacZ gene under the control of a LEF, also known as TCF (hereafter LEF/TCF) and  $\beta$ -catenin inducible promoter to report canonical Wnt signaling (Figure S1E) (DasGupta and Fuchs, 1999), showed a significant increase in the number of  $\beta$ -galactosidase-expressing cells within the adult dentate gyrus upon *sfrp3* knockdown (Figure S1E). Together, these results suggest that sFRP3 functions to suppress neural progenitor proliferation via the inhibition of Wnt signaling.

To determine whether differences in neural progenitor proliferation lead to a net change in the number of mature adult-born neurons, we injected adult mice with BrdU (50 mg/kg body weight, i.p.) once daily for 7 days and examined the expression of mature neuronal marker NeuN in BrdU<sup>+</sup> cells 28 days after the first BrdU injection (Figure 1F). The density of BrdU<sup>+</sup>NeuN<sup>+</sup> mature newborn neurons in the dentate gyrus of adult KO mice was significantly higher than that in WT littermates. Thus, sFRP3 limits neuronal production during adult hippocampal neurogenesis.

#### sFRP3 Regulates Quiescence, but Not Lineage Choice, of Dentate Radial Glia-like Neural Stem Cells

The BrdU and MCM2 results indicate that adult *sfrp3* KO mice have an increased number of intermediate precursor cells (IPCs), which constitute the large majority of dividing cells in the adult SGZ. This increase may result from changes in IPC proliferation or IPC production from RGLs. To determine the cellular target of sFRP3, we assessed RGL proliferation by identifying colocalization of MCM2 and SGZ *nestin*<sup>+</sup> cells within the adult SGZ with radial processes (Figure S2A). Stereological

quantification showed that *sfrp3* KO mice exhibited a 45% increase of activated RGLs at the population level (Figure S2B).

To directly determine whether *sfrp3* deletion affects quiescent neural stem cell activation and lineage choice in the adult SGZ, we performed short-term in vivo clonal analysis (Bonaguidi et al., 2011). We generated *nestin-CreER<sup>T2</sup>::Z/EG<sup>f/+</sup>::sfrp3<sup>-/-</sup>* (KO) and *nestin-CreER<sup>T2</sup>::Z/EG<sup>f/+</sup>::sfrp3<sup>+/+</sup>* mice (control; Figure S2C). We injected a single low dose of tamoxifen (62 mg/kg body weight, i.p.) into adult mice for induction. As shown previously, this approach sparsely labeled quiescent RGLs in the adult SGZ, and most labeled cells were MCM2<sup>-</sup> (Figure S2D) (Bonaguidi et al., 2011). At 7 days postinjection (dpi), we quantified RGL quiescence or activation status according to the absence (quiescent) or presence (active) of progeny adjacent to the RGL within individual GFP<sup>+</sup> clones (Figures 2A–2D). Adult KO mice exhibited a significant decrease in the percentage of clones with a single RGL (Figure 2E), suggesting that sFRP3 suppresses the activation of quiescent RGLs in the adult SGZ. By 7 dpi, activated RGLs could be observed generating IPCs, astroglia, or additional RGLs (Figures 2B–2D). Interestingly, the percentage of each type of activated clone was similar between WT and KO mice (Figure 2F), suggesting that *sfrp3* deletion does not alter RGL lineage choice upon activation. These results support the model that sFRP3 suppresses RGL activation in the adult dentate gyrus.

#### sFRP3 Suppresses the Tempo of Newborn Neuron Maturation in the Adult Hippocampus

Wnt signaling is known to be active in immature neurons in the adult hippocampus (Lie et al., 2005; Madsen et al., 2003); therefore, we examined whether sFRP3 also regulates newborn neuron development. The maturation status of newborn neurons can be defined by the sequential and partially overlapping expression of the immature neuron marker doublecortin (DCX) and the mature neuron marker NeuN (Figure S3A). Adult mice were injected with BrdU (50 mg/kg body weight, i.p.) once daily for 1 week and analyzed 2 weeks after the first BrdU injection. Quantitative analysis showed a significant decrease in the percentage of DCX<sup>+</sup>NeuN<sup>-</sup> immature neurons, with a concurrent increase in the percentage of more developed DCX<sup>+</sup>NeuN<sup>+</sup> neurons among all BrdU<sup>+</sup> cells in KO mice compared to WT littermates (Figures 3A–3B). Thus, *sfrp3* deletion leads to the accelerated maturation of newborn neurons in the adult dentate gyrus.

To further characterize the role of sFRP3 in neuronal development, we examined the dendritic outgrowth of newborn neurons in adult mice by using a GFP-expressing retrovirus for birth dating and genetic labeling of proliferating progenitors and their progeny (Ge et al., 2006). Quantitative analysis showed significant increases in both the total dendritic length and the branch number of GFP<sup>+</sup> newborn neurons in adult KO mice compared to WT littermates at 14 dpi (Figures 3C–3D). Interestingly, GFP<sup>+</sup> newborn neurons in the HET and KO mice exhibited similarly accelerated dendritic growth compared to WT littermates (Figures 3C–3D), suggesting that dendritic development of newborn neurons is particularly sensitive to sFRP3 levels. At 21 dpi, GFP<sup>+</sup> neurons in KO mice still exhibited significantly increased total dendritic length and branch number compared to WT littermates, although the differences were smaller compared to those at 14 dpi (Figures 3E–3F). Interestingly, GFP<sup>+</sup> neurons in KO mice also displayed significantly increased

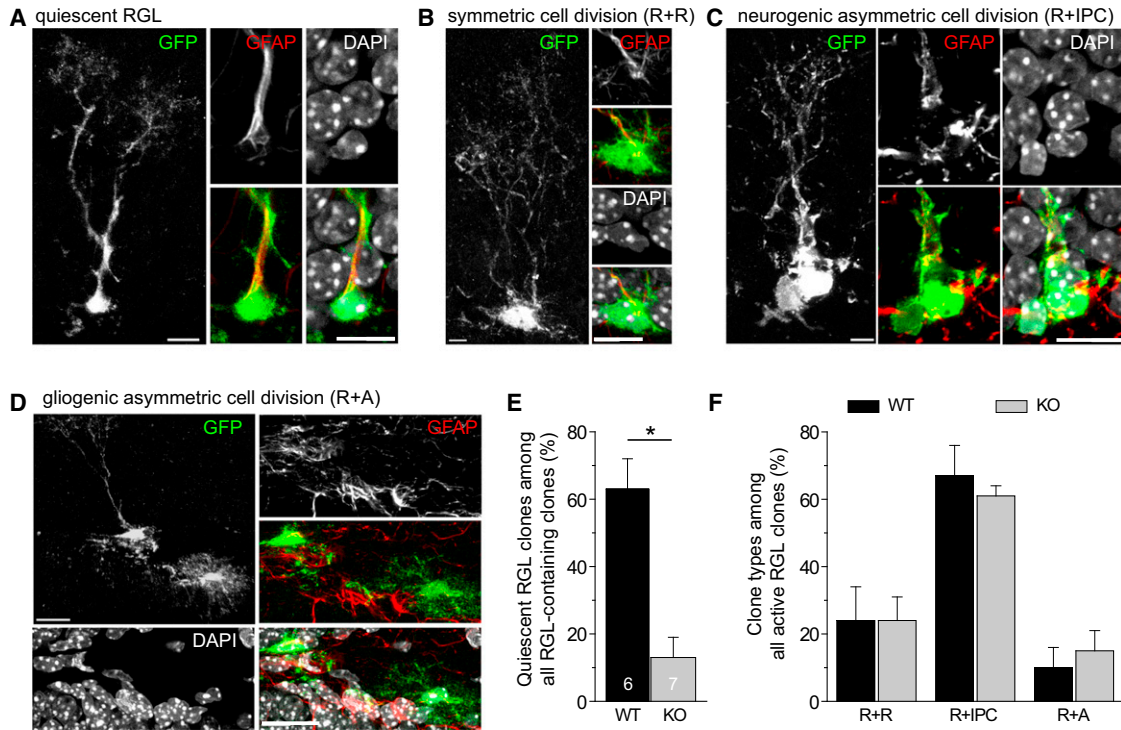


**Figure 2. Increased Activation of Quiescent Radial Glia-like Neural Stem Cells in the Dentate Gyrus of Adult *sfrp3* Knockout Mice**

(A–D) Sample confocal images of the different types of GFP<sup>+</sup> clones at 7 dpi. Adult *nestin-CreER<sup>T2/+</sup>::Z/EG<sup>f/+</sup>::sfrp3<sup>-/-</sup>* KO mice and *nestin-CreER<sup>T2/+</sup>::Z/EG<sup>f/+</sup>::sfrp3<sup>+/+</sup>* control mice were injected with a single low dose of tamoxifen (62 mg/kg body weight, i.p.) and examined 7 days later. Shown are sample confocal images of immunostaining of GFP and GFAP for a quiescent clone with a single radial glia-like neural stem cell (RGL; A) and for activated clones with two RGLs (B), one RGL and one GFAP<sup>+</sup> intermediate precursor cell (IPC; C), and one RGL and one GFAP<sup>+</sup> astrocyte with bushy morphology (A) in (D). Scale bars represent 10 μm.

(E) Decreased RGL quiescence in the dentate gyrus of adult *sfrp3* KO mice examined at 7 dpi. Values represent mean ± SEM (n = 6 WT and 7 KO mice; \*, p < 0.01; Student's t test).

(F) There was no difference in percentages of different types of activated clones in adult *sfrp3* KO mice examined at 7 dpi. Values represent mean ± SEM. The same sets of animals as in (E) were used.

See also Figure S2 and Table S1.

dendritic spine density compared to those in WT littermates at 21 dpi (Figures 3G–3H). Thus, *sfrp3* deletion leads to the increased tempo of multiple processes of neuronal maturation during adult hippocampal neurogenesis, ranging from dendritic outgrowth to dendritic spine formation of newborn neurons.

To examine whether an acute decrease in sFRP3 level also regulates newborn neurons, we stereotaxically injected lentiviruses coexpressing tdTomato and shRNA-*sfrp3* or shRNA-control and then injected retroviruses expressing GFP into the dentate gyrus of adult WT mice (Figure S3B). Analysis of GFP<sup>+</sup> newborn neurons at 14 dpi showed an increase in the total dendritic length and branch number upon shRNA-*sfrp3* expression compared to shRNA-control (Figures S3B–S3D). Few GFP<sup>+</sup> neurons were tdTomato<sup>+</sup>, further supporting a non-cell-autonomous effect of sFRP3. Together, these results suggest an inhibitory role of sFRP3 in regulating newborn neuron maturation in the adult dentate gyrus.

### sFRP3 Regulates Neuronal Activity-Induced Adult Hippocampal Neurogenesis

The activity-dependent expression profile of sFRP3 and its role in adult neurogenesis prompted us to assess whether it serves

as a substrate for activity-dependent modulation of adult neurogenesis. We examined the magnitude and time course of *sfrp3* expression in response to dentate gyrus activation by using in situ hybridization and quantitative real-time PCR analyses. The level of dentate *sfrp3* expression was reduced to about 50% of that in sham controls 1 day after ECS and gradually returned to basal levels within 7 days (Figure 4A). Exercise, a physiological stimulation that activates dentate granule neurons as indicated by immediate early gene *Arc* expression, also led to significantly decreased *sfrp3* expression (Figure 4B) and increased *Wnt* signaling (Figure S4A). To examine whether direct neuronal activation is sufficient to affect *sfrp3* expression, we stereotaxically injected engineered AAVs expressing ChR2-YFP into the adult dentate gyrus, followed by light stimulations 3 weeks later. Indeed, direct and strong activation of dentate granule neurons, as indicated by *Arc* expression, led to a significant decrease of *sfrp3* expression in the dentate granule neurons (Figure S4B). Furthermore, pathological stimulation with pilocarpine-induced seizures resulted in a prolonged decrease of *sfrp3* expression (Figure S4C). These results indicate that *sfrp3* expression in the adult dentate gyrus is regulated by multiple forms of neuronal activity in vivo.

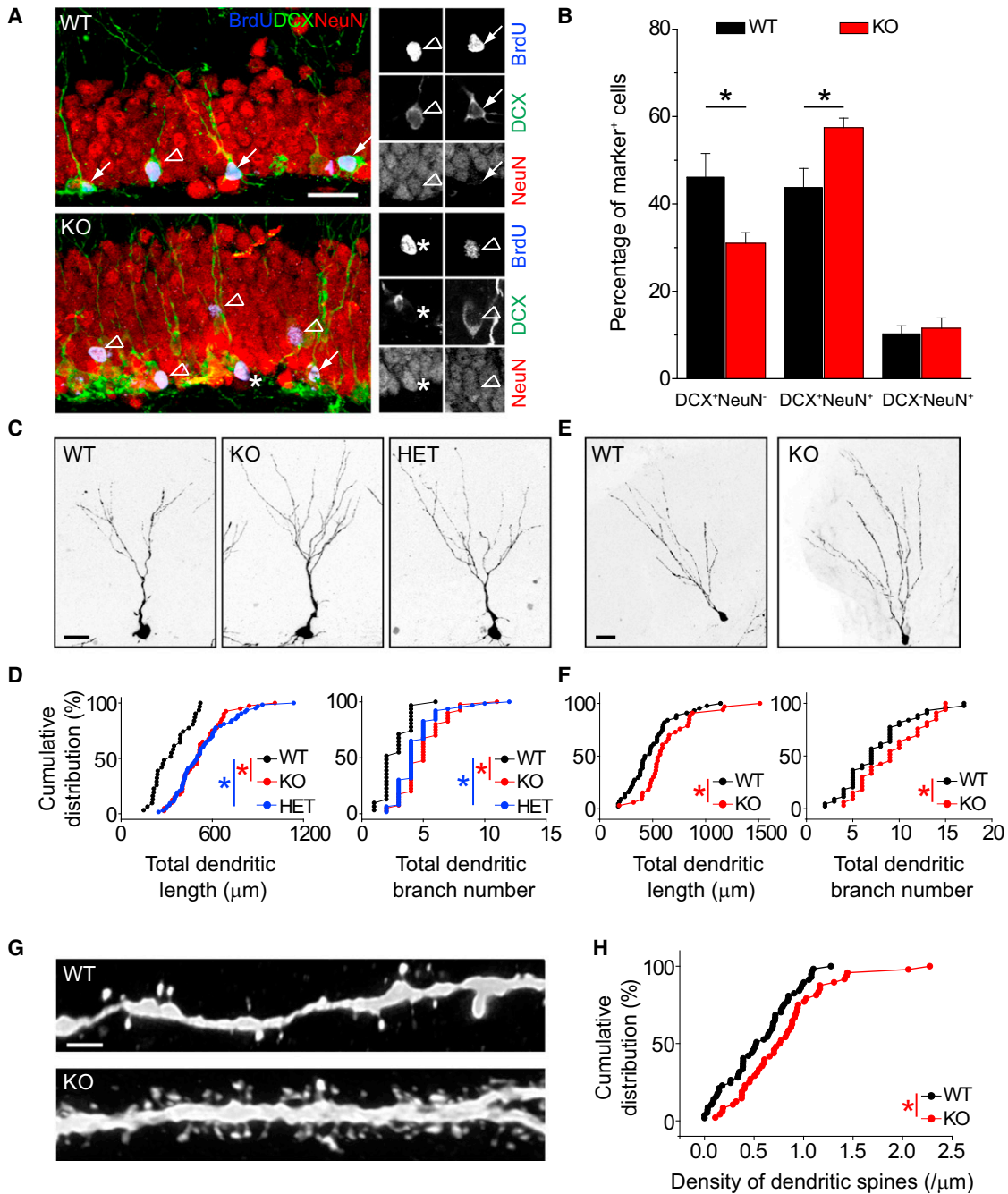


**Figure 3. Regulation of Maturation, Dendritic Development, and Spine Formation of Newborn Neurons in the Adult Hippocampus by sFRP3** (A and B) Accelerated new neuron maturation in the dentate gyrus of adult *sfrp3* KO mice. Adult mice were injected with BrdU once daily for 1 week and analyzed 2 weeks after the first BrdU injection. Shown in (A) are sample confocal images of BrdU, DCX, and NeuN immunostaining. Arrows point to BrdU<sup>+</sup>DCX<sup>+</sup>NeuN<sup>-</sup> immature newborn neurons, arrowheads point to BrdU<sup>+</sup>DCX<sup>+</sup>NeuN<sup>+</sup> more developed newborn neurons, and asterisks point to BrdU<sup>+</sup>DCX<sup>-</sup>NeuN<sup>+</sup> mature new neurons. Scale bar represents 20 μm. Shown in (B) is a summary of the distribution of newborn neurons at different maturation stages. Values represent mean ± SEM (n = 9 animals in each group; \*, p < 0.01; one-way ANOVA). (C–H) Accelerated dendritic growth and spine formation of newborn neurons in the dentate gyrus of adult *sfrp3* KO mice. Retroviruses expressing GFP were stereotaxically injected into the dentate gyrus of adult *sfrp3* KO, HET, and WT littermates. GFP<sup>+</sup> neurons were examined at 14 dpi (C and D) or 21 dpi (E–H). Shown are sample projected confocal images of GFP<sup>+</sup> newborn neurons at 14 dpi (C) and 21 dpi (E) and dendritic spines at 21 dpi (G). Scale bars represent 20 μm. Also shown are cumulative distribution plots of total dendritic length, branch number, and spine density of newborn neurons under different conditions (D, F, and H). Each symbol represents data from a single GFP<sup>+</sup> neuron (\*, p < 0.01, Kolmogorov-Smirnov test; n = 3 animals each). See also Figure S3 and Table S1.

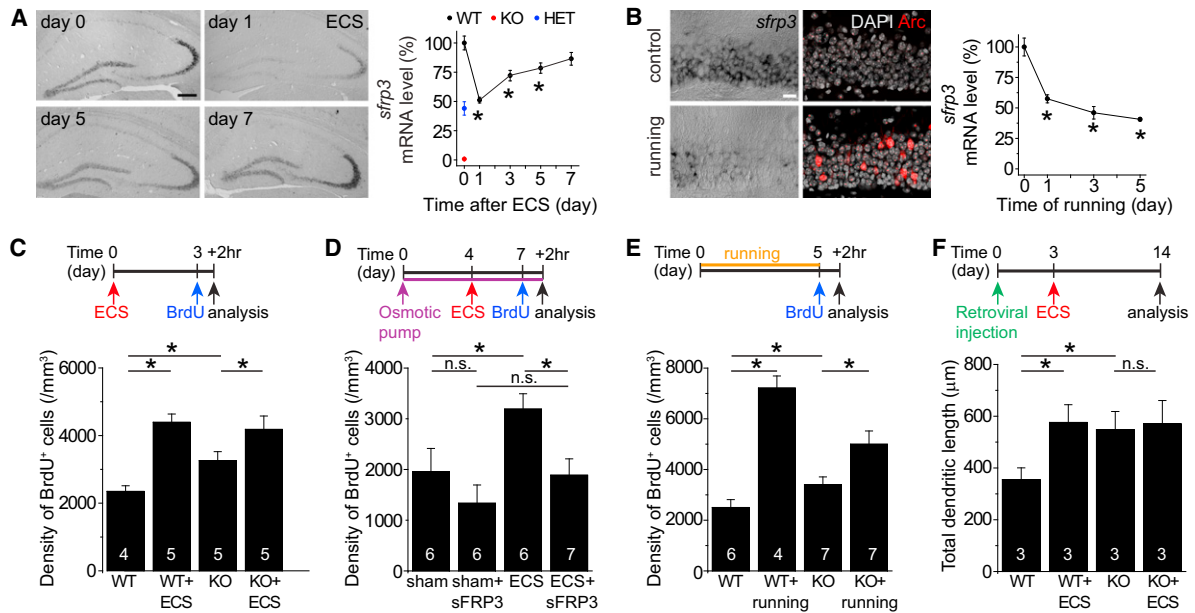


**Figure 4. *sfrp3* Reduction of *sfrp3* Mediates Activity-Dependent Adult Neurogenesis**

(A) ECS decreases *sfrp3* expression in the adult dentate gyrus. Shown are sample images of *sfrp3* in situ in the adult hippocampus at different times after a single ECS (left; scale bar represents 200 μm) and quantification by quantitative real-time PCR. Values are normalized to that of sham-treated WT animals at each time point and represent mean ± SEM (n ≥ 3 animals for each time point; \*, p < 0.01; Student's t test).

(B) Running activates dentate granule neurons and decreases *sfrp3* expression. Shown are sample images of dual *sfrp3* in situ and Arc immunostaining (left; scale bar represents 20 μm) and quantification by quantitative real-time PCR (right). Values are normalized to that of sham-treated WT animals and represent mean ± SEM (n ≥ 3 animals for each time point; \*, p < 0.01; Student's t test).

(C) *sfrp3*-deletion-induced increase of progenitor proliferation significantly occludes the ECS effect in the adult SGZ. Shown are schematic diagrams of experimental designs and a stereological quantification of BrdU+ cells in the adult SGZ after a single ECS. Values represent mean ± SEM (\*, p < 0.05; one-way ANOVA).

(D) Exogenous sFRP3 blocks ECS-induced neural progenitor proliferation in adult WT mice. Shown are schematic diagrams of experimental designs and a stereological quantification of BrdU+ cells in the adult SGZ under different conditions. Values represent mean ± SEM (\*, p < 0.05; n.s., p > 0.1; one-way ANOVA).

(E) Running-induced increase of cell proliferation is attenuated in the adult *sfrp3* KO mice. Similar to (C), except mice were subjected to voluntary running.

(F) *sfrp3*-deletion-induced dendritic growth of newborn neurons completely occludes the ECS effect. Similar to (C), except the dendritic growth of retrovirally labeled new neurons was analyzed at 14 dpi.

See also Figure S4 and Table S1.

Next, we examined the impact of *sfrp3* deletion on the sequential steps of adult neurogenesis in response to dentate gyrus activation. We subjected adult *sfrp3* KO mice and their WT littermates to a single ECS and analyzed progenitor proliferation with BrdU injection 3 days later (Figure 4C). Interestingly, the ECS-induced increase of progenitor proliferation was attenuated from 87% in WT mice to 28% in *sfrp3* KO littermates (Figures 4C and S4D), suggesting significant occlusion of the ECS-induced increase of progenitor proliferation by *sfrp3* deletion. Notably, the lack of further increase by ECS in adult *sfrp3* KO mice was not due to a ceiling effect on progenitor proliferation, because WT mice exhibited an even higher number of BrdU+ cells after running (Figure 4E). Importantly, infusion of recombinant sFRP3 protein into the dentate gyrus of adult WT mice abolished the ECS-induced increase of neural progenitor proliferation (Figure 4D), suggesting that a reduction of sFRP3 levels is required for the ECS-induced increase of progenitor proliferation. In addition to the results from ECS, we also observed that the voluntary-running-induced increase of progenitor proliferation was attenuated from 188% in WT mice to 47% in KO littermates (Figures 4E and S4E). Together, these results suggest that

sFRP3, at least in part, mediates activity-induced neural progenitor proliferation in the adult dentate gyrus.

To address whether *sfrp3* is also involved in ECS-induced acceleration of new neuron development during adult neurogenesis, we subjected WT mice to a single ECS either 3 or 6 days after retroviral injection. Morphological assessment at 14 dpi demonstrated that ECS at both time points increased the total dendrite length and branch number of GFP+ newborn neurons (Figures S4F–S4G). In contrast, ECS had no effect on dendritic growth of GFP+ newborn neurons in adult *sfrp3* KO mice (Figures 4F and S4H). Thus, *sfrp3* deletion also occludes activity-induced acceleration of new neuron dendritic development in the adult dentate gyrus.

## DISCUSSION

Two fundamental questions in stem cell biology are whether niche signals couple changing tissue demands with somatic stem cell activity to promote functional homeostasis and how they might do it. Unique among adult somatic tissues, neural stem cells reside within an active neuronal network where the

local neuronal activity could serve as an effective readout of current tissue demands and provide signals to tune the magnitude and tempo of neurogenesis. Our study identifies sFRP3 as a neuronal-activity-regulated niche factor from mature dentate granule neurons that exhibits control over multiple steps of adult hippocampal neurogenesis, including the activation of quiescent adult neural stem cells, maturation, dendritic development, and spine formation of newborn dentate granule neurons. Our results suggest a significant mode of dynamic regulation of adult neurogenesis via the acute release of tonic inhibition.

Little is known about niche mechanisms regulating quiescent neural stem cells, largely because of a lack of effective approaches for examining this population of precursors. Using a genetic sparse-labeling approach for clonal analysis of stem cell division and lineage choice (Bonaguidi et al., 2011), we show that sFRP3 deletion increases quiescent neural stem cell activation in the adult hippocampus and, surprisingly, has no effect on the frequency of symmetric and asymmetric neurogenic or gliogenic cell division. Thus, in contrast to a prominent role of Wnt signaling in promoting neuronal fate commitment of proliferating multipotent adult neural progenitors in vitro (Lie et al., 2005), sFRP3 does not affect the lineage choice of quiescent RGLs within the adult hippocampus in vivo. Interestingly, sFRP3 inhibits both quiescent neural stem cell activation and the maturation of their neuronal progeny. This activity-driven, coordinated regulation of sequential processes suggests that sFRP3 may be both a sensor and an effector for the homeostatic regulation of adult neurogenesis.

While Wnt signaling has been shown to control the proliferation and differentiation of progenitors in many adult tissues (Clevers and Nusse, 2012), little is known about the in vivo functions of the various naturally secreted Wnt inhibitors in adult stem cell biology. Consistent with a role as a broad Wnt signaling inhibitor in the adult brain, sFRP3 reduction leads to increased canonical Wnt signaling in the adult dentate gyrus, as indicated by TOPGAL reporter activation. Interestingly, endogenous *sfrp3* expression in the dentate gyrus is reduced by therapeutic (ECS), physiological (voluntary running), and pathological (seizures) stimuli as well as direct neuronal activation, suggesting that sFRP3 is a key sensor of various external stimuli within the dentate granule neurons in vivo. Similar to our findings on *sfrp3*, an independent study showed that the loss of Dkk1 in neural progenitors in the adult dentate gyrus leads to increased cell proliferation and the acceleration of newborn neuron development (Seib et al. 2013, this issue), suggesting a common role among different Wnt inhibitors in adult neurogenesis. The presence of potent negative regulators, such as sFRP3 and Dkk1, may also be of significant physiological importance in keeping the process of adult neurogenesis in balance. For example, pathological activation of neuronal circuitry by chronic seizures, which leads to a sustained decrease in *sfrp3* expression, causes the aberrant outgrowth of newborn neurons and the formation of recurrent connections that may contribute to epileptogenesis (Jessberger et al., 2007; Parent et al., 1997). Recent studies have also suggested significant depletion of neural stem cells upon their activation in the adult dentate gyrus (Bonaguidi et al., 2012). For example, the deletion of BMPR1A or SMAD4, PTEN, RBPJ $\kappa$ , or REST (also known as NRSF) in adult neural stem cells leads to the initial

activation and subsequent depletion of the stem cell pool and reduced levels of continuous adult hippocampal neurogenesis. Therefore, a tightly controlled dynamic range of Wnt signaling via inhibitor levels may fine tune adult neural stem cell behavior to meet changing local tissue demands while globally maintaining the stem cell pool over the long term—a mechanism that may be generalizable to the regulation of other stem cells.

In summary, our study suggests a model in which physiological experience and pathological stimuli, via neuronal activity, modulate *sfrp3* expression in dentate granule neurons to regulate quiescent neural stem cell activation and the development of their progeny by fine tuning Wnt signaling. Given the critical contribution of adult neurogenesis to brain plasticity, learning and memory, and brain disorders, the identification of sFRP3 as an activity-dependent inhibitory niche factor has significant and broad implications.

## EXPERIMENTAL PROCEDURES

### RNA-Seq, Quantitative Real-Time PCR, and In Situ Hybridization

Total poly-A-containing messenger RNA was immediately isolated after the dissection of the dentate gyrus from hippocampi to create the complementary DNA (cDNA) library for HiSeq2000 sequencing (Illumina). Paired-end reads (97 bp) of cDNA sequences were aligned to the mouse reference genome mm9 by TopHat47 with reference gene annotations. The relative abundances of each transcript were estimated by Cufflinks48 with Ensembl gene annotation (build NCBIM37).

Quantitative real-time PCR was performed in triplicate with the following primers: GAPDH: 5'-GTATTGGGCGCCTGGTACC-3' (forward), 5'-CGC TCCTGGAAGATGGTGATGG-3' (reverse); sFRP3: 5'-CAAGGGACACCGTCAA TCTT-3' (forward), 5'-CATATCCCAGCGCTTGACTT-3' (reverse).

In situ hybridization analysis was performed with the use of the digoxigenin-labeled antisense RNA corresponding to the full-length coding sequence of *sfrp3*, as previously described (Ma et al., 2009). All experiments were processed in parallel for the direct comparison of labeling.

### Electroconvulsive Stimulation, Voluntary Running, Pilocarpine Treatment, and Optogenetic Manipulation

Animals were administered ECS as previously described (Ma et al., 2009). Sham control animals received the same treatment, except no current was passed. For voluntary-running experiments, animals were randomly separated into two groups in standard home cages with free access to a functional or locked running wheel mounted in the cage as described previously (Guo et al., 2011a; Ma et al., 2009). For pilocarpine-induced seizure, adult female WT mice were i.p. administered methylscopolamine (2 mg/kg body weight), followed by pilocarpine (320 mg/kg body weight) 30 min later. Control mice were administered a comparable volume of vehicle after the initial methylscopolamine treatment. Only mice that had multiple level III–V seizures within 2 hr of pilocarpine injection were used (Shibley and Smith, 2002). For optogenetic manipulation, fiber optic cannulae (Doric Lenses) were implanted at the same sites right after AAV injection with a dorsal-ventral depth of 1.6 mm from the skull and mice were left to recover for three weeks, as previously described (Song et al., 2012). A light-stimulation protocol (472 nm; 15 ms at 20 Hz for 3 min) (Liu et al., 2012) was applied via the DPSSL Laser System (Laser Century) two times 4 days apart, similarly as previously described (Song et al., 2012). Animals were processed for dual *sfrp3* in situ and Arc immunostaining 2 hr after the second light stimulation. All animal procedures were approved by the Institutional Animal Care and Use Committee.

### BrdU Labeling, Immunostaining, Confocal Imaging, and Analysis

Adult littermates of adult female *sfrp3* WT and KO mice (7–8 weeks old) were i.p. injected once with BrdU (200 mg/kg body weight) and analyzed 2 hr later. For neuronal differentiation and maturation analysis, adult littermates were injected with BrdU (50 mg/kg body weight, once daily at 10 a.m.) for 1 week and sacrificed 2 or 4 weeks after the first BrdU injection. Coronal brain sections (40  $\mu$ m thick) were prepared from injected mice and processed for immunostaining

and confocal imaging as previously described (Bonaguidi et al., 2011; Ge et al., 2006). Antibodies used in this study are listed in Table S1. Stereological quantification within the SGZ and granule cell layer was carried out as previously described (Kempermann et al., 1997). All assessments were performed by an observer blind to genotypes or treatments. Statistical significance ( $p < 0.01$ ) was assessed with a one-way ANOVA or Student's *t* test, as indicated.

#### Production and Stereotaxic Injection of Engineered Viruses, and Osmotic Pump Infusion

Engineered self-inactivating murine oncoretroviruses were used to express GFP specifically in proliferating cells and their progeny after stereological injection and were processed at 14 or 21 dpi for morphological analysis as previously described (Ge et al., 2006). Summaries of the total dendritic length, branch number, and spine density of each individual neuron under different conditions are shown in cumulative distribution plots. Statistical significance ( $p < 0.01$ ) was assessed with the Kolmogorov-Smirnov test.

Lentiviruses that coexpress shRNA under the U6 promoter and tdTomato under the EF1 $\alpha$  promoter were stereotaxically injected into the dentate gyrus of adult WT mice. The short hairpin sequences used are as follows: shRNA-*sfrp3*, 5'-GCTAGCGATTCCACTCAGAAT-3'; shRNA-control, 5'-AGTTCCAGTACGGCTCCAA-3'. For cell-proliferation analysis, BrdU (200 mg/kg body weight) was injected 14 days after lentiviral infection and examined 2 hr later. Stereological quantification of BrdU<sup>+</sup> cells in the SGZ was carried out only in tdTomato<sup>+</sup> coronal sections. For dendritic-development analysis, retroviruses expressing GFP were injected into the same sites 14 days after lentiviral injection, and mice were examined 14 days later for morphological analysis. An AAV vector coexpressing the same shRNA under the U6 promoter and GFP under the EF1 $\alpha$  promoter (Guo et al., 2011b) was used in adult TOPGAL reporter mice for the examination of the role of sFRP3 in Wnt signaling.

For optogenetic manipulation, engineered AAVs that express ChR2-YFP under the EF1 $\alpha$  promoter were obtained from the Viral Core of University of Pennsylvania and stereotaxically injected into the dentate gyrus of adult WT mice with the following coordinates: posterior = -2 mm from Bregma; lateral =  $\pm$  1.5 mm; ventral = 2.2 mm.

For sFRP0-infusion experiments, adult WT animals were infused with recombinant sFRP3 (120 ng/day; R&D Systems) into the right ventricle by osmotic minipumps (Alzet) for 7 days with the following coordinates: posterior = 0.34 mm from Bregma, lateral = 1 mm, ventral = 3 mm (Guo et al., 2011a). Animals were subjected to a single ECS on day 4, injected with BrdU (200 mg/kg body weight) on day 7, then analyzed 2 hr after BrdU injection.

#### Animals, Tamoxifen Administration, and Clonal Analysis

TOPGAL reporter mice (DasGupta and Fuchs, 1999) were used for the monitoring of canonical Wnt signaling. Nestin-GFP mice (Song et al., 2012) were used for the dual *sfrp3* in situ and GFP immunohistology analysis. For clonal analysis, *nestin-CreER<sup>T2+/-</sup>::Z/EG<sup>f/+</sup>::sfrp3<sup>-/-</sup>* mice and *nestin-CreER<sup>T2+/-</sup>::Z/EG<sup>f/+</sup>::sfrp3<sup>+/+</sup>* control mice were used. A single low dose of tamoxifen injection (62 mg/kg body weight, i.p.; Sigma) into 2-month-old mice resulted in sparse labeling at the clonal level for analysis at 7 dpi in both control and *sfrp3* KO mice, as previously described (Bonaguidi et al., 2011).

#### SUPPLEMENTAL INFORMATION

Supplemental Information contains Supplemental Experimental Procedures, four figures, and one table and can be found with this article online at <http://dx.doi.org/10.1016/j.stem.2012.11.021>.

#### ACKNOWLEDGMENTS

We thank Drs. D. Ginty, S. Jessberger, X. He, and members of the Song and Ming laboratories for their suggestions, A. Rattner and J. Nathans for generating *sfrp3* KO mice, J.H. Shin and B. Xie for help with RNA-seq, and P. Worley for Arc antibodies and initial help with ECS. This work was supported by the NIH (NS047344, MH087874, and ES021957 to H.S.; NS048271 and HD069184 to G.M.; MH090115 to M.-H.J.; and NS080913 to M.A.B) and NARSAD (Independent Investigator awards to H.S. and G.-I.M., and a Young

Investigator award to M.-H.J.) and by postdoctoral fellowship awards from MSCRF to J.S., E.K., Y.S., and K.C.

Received: June 5, 2012

Revised: October 19, 2012

Accepted: November 19, 2012

Published: February 7, 2013

#### REFERENCES

- Bonaguidi, M.A., Wheeler, M.A., Shapiro, J.S., Stadel, R.P., Sun, G.J., Ming, G.L., and Song, H. (2011). In vivo clonal analysis reveals self-renewing and multipotent adult neural stem cell characteristics. *Cell* 145, 1142–1155.
- Bonaguidi, M.A., Song, J., Ming, G.L., and Song, H. (2012). A unifying hypothesis on mammalian neural stem cell properties in the adult hippocampus. *Curr. Opin. Neurobiol.* 22, 754–761.
- Bracko, O., Singer, T., Aigner, S., Knobloch, M., Winner, B., Ray, J., Clemenson, G.D., Jr., Suh, H., Couillard-Despres, S., Aigner, L., et al. (2012). Gene expression profiling of neural stem cells and their neuronal progeny reveals IGF2 as a regulator of adult hippocampal neurogenesis. *J. Neurosci.* 32, 3376–3387.
- Clevers, H., and Nusse, R. (2012). Wnt/ $\beta$ -catenin signaling and disease. *Cell* 149, 1192–1205.
- DasGupta, R., and Fuchs, E. (1999). Multiple roles for activated LEF/TCF transcription complexes during hair follicle development and differentiation. *Development* 126, 4557–4568.
- Ge, S., Goh, E.L., Sailor, K.A., Kitabatake, Y., Ming, G.L., and Song, H. (2006). GABA regulates synaptic integration of newly generated neurons in the adult brain. *Nature* 439, 589–593.
- Guo, J.U., Ma, D.K., Mo, H., Ball, M.P., Jang, M.H., Bonaguidi, M.A., Balazer, J.A., Eaves, H.L., Xie, B., Ford, E., et al. (2011a). Neuronal activity modifies the DNA methylation landscape in the adult brain. *Nat. Neurosci.* 14, 1345–1351.
- Guo, J.U., Su, Y., Zhong, C., Ming, G.L., and Song, H. (2011b). Hydroxylation of 5-methylcytosine by TET1 promotes active DNA demethylation in the adult brain. *Cell* 145, 423–434.
- Jessberger, S., Zhao, C., Toni, N., Clemenson, G.D., Jr., Li, Y., and Gage, F.H. (2007). Seizure-associated, aberrant neurogenesis in adult rats characterized with retrovirus-mediated cell labeling. *J. Neurosci.* 27, 9400–9407.
- Jessberger, S., Clark, R.E., Broadbent, N.J., Clemenson, G.D., Jr., Consiglio, A., Lie, D.C., Squire, L.R., and Gage, F.H. (2009). Dentate gyrus-specific knockdown of adult neurogenesis impairs spatial and object recognition memory in adult rats. *Learn. Mem.* 16, 147–154.
- Jones, S.E., and Jomary, C. (2002). Secreted Frizzled-related proteins: searching for relationships and patterns. *Bioessays* 24, 811–820.
- Kempermann, G., Kuhn, H.G., and Gage, F.H. (1997). More hippocampal neurons in adult mice living in an enriched environment. *Nature* 386, 493–495.
- Lie, D.C., Colamarino, S.A., Song, H.J., Désiré, L., Mira, H., Consiglio, A., Lein, E.S., Jessberger, S., Lansford, H., Dearie, A.R., and Gage, F.H. (2005). Wnt signalling regulates adult hippocampal neurogenesis. *Nature* 437, 1370–1375.
- Liu, X., Ramirez, S., Pang, P.T., Puryear, C.B., Govindarajan, A., Deisseroth, K., and Tonegawa, S. (2012). Optogenetic stimulation of a hippocampal engram activates fear memory recall. *Nature* 484, 381–385.
- Ma, D.K., Jang, M.H., Guo, J.U., Kitabatake, Y., Chang, M.L., Pow-Anpongkul, N., Flavell, R.A., Lu, B., Ming, G.L., and Song, H. (2009). Neuronal activity-induced Gadd45b promotes epigenetic DNA demethylation and adult neurogenesis. *Science* 323, 1074–1077.
- Madsen, T.M., Treschow, A., Bengzon, J., Bolwig, T.G., Lindvall, O., and Tingström, A. (2000). Increased neurogenesis in a model of electroconvulsive therapy. *Biol. Psychiatry* 47, 1043–1049.
- Madsen, T.M., Newton, S.S., Eaton, M.E., Russell, D.S., and Duman, R.S. (2003). Chronic electroconvulsive seizure up-regulates beta-catenin expression in rat hippocampus: role in adult neurogenesis. *Biol. Psychiatry* 54, 1006–1014.

Ming, G.L., and Song, H. (2011). Adult neurogenesis in the mammalian brain: significant answers and significant questions. *Neuron* 70, 687–702.

Miranda, C.J., Braun, L., Jiang, Y., Hester, M.E., Zhang, L., Riolo, M., Wang, H., Rao, M., Altura, R.A., and Kaspar, B.K. (2012). Aging brain microenvironment decreases hippocampal neurogenesis through Wnt-mediated survivin signaling. *Aging Cell* 11, 542–552.

Overstreet-Wadiche, L.S., Bromberg, D.A., Bensen, A.L., and Westbrook, G.L. (2006). Seizures accelerate functional integration of adult-generated granule cells. *J. Neurosci.* 26, 4095–4103.

Parent, J.M., Yu, T.W., Leibowitz, R.T., Geschwind, D.H., Sloviter, R.S., and Lowenstein, D.H. (1997). Dentate granule cell neurogenesis is increased by seizures and contributes to aberrant network reorganization in the adult rat hippocampus. *J. Neurosci.* 17, 3727–3738.

Seib, D.R.M., Corsini, N.S., Ellwanger, K., Plaas, C., Mateos, A., Pitzer, C., Niehrs, C., Celikel, T., and Martin-Villalba, A. (2013). Loss of Dickkopf-1 restores neurogenesis in old age and counteracts cognitive decline. *Cell Stem Cell* 12, this issue, 204–214.

Shibley, H., and Smith, B.N. (2002). Pilocarpine-induced status epilepticus results in mossy fiber sprouting and spontaneous seizures in C57BL/6 and CD-1 mice. *Epilepsy Res.* 49, 109–120.

Shimogori, T., VanSant, J., Paik, E., and Grove, E.A. (2004). Members of the Wnt, Fz, and Frp gene families expressed in postnatal mouse cerebral cortex. *J. Comp. Neurol.* 473, 496–510.

Song, H., Stevens, C.F., and Gage, F.H. (2002). Astroglia induce neurogenesis from adult neural stem cells. *Nature* 417, 39–44.

Song, J., Zhong, C., Bonaguidi, M.A., Sun, G.J., Hsu, D., Gu, Y., Meletis, K., Huang, Z.J., Ge, S., Enikolopov, G., et al. (2012). Neuronal circuitry mechanism regulating adult quiescent neural stem-cell fate decision. *Nature* 489, 150–154.

Thompson, C.L., Pathak, S.D., Jeromin, A., Ng, L.L., MacPherson, C.R., Mortrud, M.T., Cusick, A., Riley, Z.L., Sunkin, S.M., Bernard, A., et al. (2008). Genomic anatomy of the hippocampus. *Neuron* 60, 1010–1021.

Zhao, C., Warner-Schmidt, J., Duman, R.S., and Gage, F.H. (2012). Electroconvulsive seizure promotes spine maturation in newborn dentate granule cells in adult rat. *Dev. Neurobiol.* 72, 937–942.